Printed ISSN 1330–0008
Online ISSN 1333–9125
CD ISSN 1333–8390
CODEN FIZAE4

COHERENT CONTROL OF SPONTANEOUS EMISSION SPECTRUM IN A DOUBLY DRIVEN Y-TYPE ATOM

BIBHAS KUMAR DUTTA[a,1] and PRASANTA KUMAR MAHAPATRA[b]

[a]*Department of Physics, J. K. College, Purulia 723 101, India*

[b]*Department of Physics and Technophysics, Vidyasagar University, Midnapore 721 102, India*

Received 1 February 2009; Revised manuscript received 8 November 2010
Accepted 9 February 2011 Online 15 April 2011

We have studied the dynamic control of the spontaneous emission spectrum in a Y-type atomic system driven by two coherent fields. In different dynamic conditions, the evolution of coherent spectral features in the bare-state model, has been analyzed by using the dressed-state model. For the system under purely dissipative environment, it has been shown that the behaviour of spectral components can be coherently controlled by changing the values of the Rabi frequencies and detunings of external fields. At the condition of resonant evolution of spectra, present work highlights that the emission line shape can be strongly modified for unequal decay rates of the uppermost doublet states. In this situation, the phenomenon of constructive quantum interference gives rise to the emergence of a single peak at a certain spectral position when two distinct peaks disappear at the other spectral positions. Owing to the mutual orientation of polarizations of the fields interacting with the atom in a specific configuration, we have incorporated the static phase-variation effect to exhibit phase-dependent spectra. We consider the present model with a typical field configuration such that the frequency mismatch between two coherent fields introduces the dynamic phase-variation effect. This phenomenon leads to obtain anomalous peak-shifting effect accompanied by the selective quenching of emission within the spectral profile.

PACS numbers: 42.50.Ct, 32.80.Qk, 32.50.+d UDC 539.184, 539.186

Keywords: doubly driven Y-type atom, dynamic control of coherent spectral features, incoherent elimination of spectral component, dependence of the line intensity on the incoherent pumping rate, static and dynamic phase-variation effects, phase-dependent emission spectra, anomalous peak shifting effect

[1]Corresponding author

1. Introduction

Over the past two decades, much attention has been paid to the study of effects of quantum interference arising from the interaction between atomic transition pathways [1 − 3]. The phenomenon of destructive quantum interference plays a vital role in quantum optical effects like electromagnetically induced transparency (EIT) [2, 4], gain without population inversion (GWI) or lasing without inversion (LWI) [5] and enhancement of refractive index [6]. In ideal three-level schemes (Λ, V and Ξ), such coherency effects can be obtained by applying the external coherent fields and can be dynamically controlled by changing the amplitudes and detunings of the fields. In four-level schemes, incorporation of an extra coherent field considerably changes the optical properties and leads to a number of interesting phenomena like two-photon inhibition [7] and enhancement [8], photon switching [9], non-linear light generation [10], spontaneous emission cancellation [11 − 15]. Modification and control of spontaneous emission is an active research topic in the recent years as the suppression of spontaneous emission reduces the limit of quantum-noise. Further, the quenching of spontaneous emission on some atomic transition will facilitate to achieve a population inversion on this transition using a very weak incoherent pumping. Thus, the control of spontaneous emission can be potentially useful to construct lasers in the high-frequency domain. Coherent control of spontaneous emission in an atom which is near-resonant with the edge of a photonic band gap, opens up the possibility to realize a single-atom optical memory device [16]. These facts motivate us to study the dynamic control of the behaviour of spontaneous emission in a doubly driven four-level Y-type atomic system. Among the four-level schemes, the Y-type schemes have attracted a lot of attention [7, 17 − 20]. Present Y-type model with different field configurations has not yet been studied for the purpose of controlling the spontaneous emission spectrum. In order to make our study more plausible, we need to review briefly the earlier studies regarding spontaneous emission modification in different level-schemes.

Fontana and Srivastava [21] predicted the appearance of a spectral 'hole' in the spontaneous emission spectrum of a three-level atom whose one excited level is nondecaying and coherently coupled by a static field to another excited level. Twenty-two years later, for a sinusoidal coupling field in a similar Ξ-type system, the dark line in the spontaneous emission spectrum has been explained by Zhu et al. [22] from the standpoint of destructive quantum interference. Similar works [23 − 25] based on this field-induced interference effect, have been performed in different three-level schemes. Apart from the dynamically induced coherence controlling of the spectrum, other types of coherence-like vacuum-induced coherence (VIC) or spontaneously generated coherence (SGC) [26] have been employed in various level-schemes [27 − 31] to exhibit the phenomena like spontaneous emission cancellation, suppression of spectral components and spectral narrowing. However, the occurrence of VIC requires a stringent condition under which two transition dipole matrix elements corresponding to the interfering decay channels should be non-orthogonal. Still now, such a condition is experimentally [32] found to exist in molecule-like sodium dimer, but not in other atomic systems. Since, the orthogonal dipoles for two transitions to the excited states with very small energy separation are more easily found in nature, there is a need to find different mechanism which is beyond the condition of non-orthogonality. Depending upon multiple decay-interference mechanisms [33, 34], in folded-type atomic configurations, attempts have been made by different authors [12 − 15, 35, 36] to generate the coherency effects in the spontaneous emission spectrum. In contrast to the earlier investigations regarding spontaneous emission modification, in this work, we study the evolution of spectra for appreciable values of incoherent pumping rates and the coherence decay rates involved in the field-induced transition channels. The dynamic control of spontaneous emission spectrum in our Y-type model is shown within both the non-dissipative and purely dissipative environments. On controlling the emission spectra, the static and dynamic phase-variation effects are introduced in the given model.

The salient features of the work presented in this paper are listed as follows. i) We study the coherent features in the present model at different conditions of detunings and Rabi frequencies of the external fields when the spectral line shapes are not affected by the dissipative factors. The evolution of coherent spectral features in the bare-state model, has been analyzed by using the dressed-state model. Dressed-state interpretation leads us to obtain the limiting values of the subnatural linewidths of the emission peaks in different cases. ii) It has been predicted that for coherent superposition of the uppermost excited states at the initial moment, the total cancellation of emission over the whole spectral range is possible when the incoherency effects are absent in the system. iii) Considering the system under purely dissipative environment, for different dynamic conditions, we discuss the coherent control of the spectral behaviours. The required conditions of achieving subnatural linewidths of the spectral lines are also discussed. iv) It is shown that at the condition of equal and opposite detuning of the coherent fields, three-peak spectrum will occur with asymmetric peak-widths when decay rates of the uppermost excited doublet are unequal. v) For unequal decay rates of the excited doublet, we also show that the phenomenon of constructive quantum interference can strongly modify the emission line shape at the condition of non-resonant detuning of the fields. In such a condition, due to this phenomenon of quantum interference, two distinct peaks disappear at their spectral positions and a new peak results in the line shape at a different spectral position. vi) For non-resonant evolution of emission peaks, it is found that symmetric change in peak-distribution may occur within the line shape by incoherent means. vii) We show the dependence of the line intensities on the incoherent pumping rate. viii) On inclusion of the static phase-variation effect arising from the mutual orientation of polarizations of the field vectors in our model with a specific field configuration, we also study the phase-dependent switching of the spectral lines. Phase tuned spontaneous emission spectrum can exhibit a narrow structure. ix) For frequency mismatch between two coherent fields, the emission spectrum can be further controlled by introducing the effect of dynamic phase variation which gives rise to anomalous peak-shifting effect along with the selective quenching of emission.

2. A four-level Y-type model

We consider an ideal four-level Y-type atom as shown in Fig. 1a. Two upper levels $|3\rangle$ and $|4\rangle$ are coupled to the lower level $|2\rangle$ by the single-mode driving fields $E(\omega_2)$ and $E(\omega_1)$, respectively. Here ω_1 and ω_2 are their frequencies. The atom-field coupling constants are accordingly named as g_1 and g_2. The energy level $|2\rangle$ can spontaneously radiate to the level $|1\rangle$ due to the interaction with the vacuum modes and their coupling constant is denoted as g_k where k represents both the wave-vector and polarization of the vacuum modes [37].

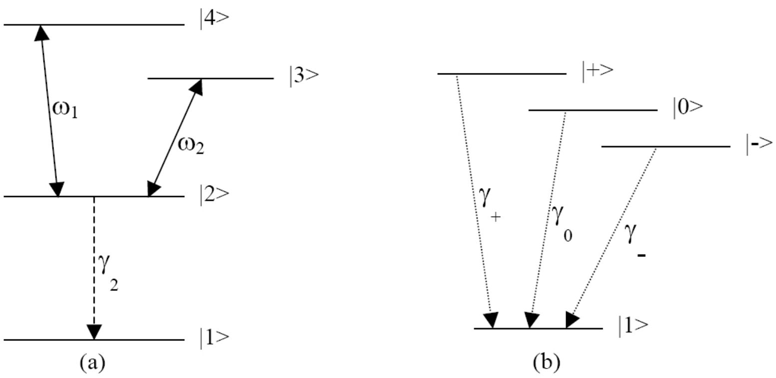

Fig. 1. Schematic diagram of an ideal four-level Y-type system interacting with two coherent fields designated by their frequencies ω_1 and ω_2 (a) in the bare-state picture (γ_2 denotes the spontaneous decay rates of the excited level $|2\rangle$), (b) in the dressed-state picture of both coupling fields. $\gamma_\pm$ and γ_0 are the decay rates of the dressed excited triplet-states $|\pm\rangle$ and $|0\rangle$, respectively.

2.1. Theoretical formulation

The total Hamiltonian of the system can be written as

$$H = H_o + H' \,, \tag{1}$$

where H_o includes the independent contributions of the atom and the field systems and H' includes the perturbation effect of the external fields on the atom. The Hamiltonian H_o can be expressed as

$$H_o = H_A + H_F + H_V \,, \tag{2}$$

where H_A, H_F and H_V represent the Hamiltonians for the atom, driving fields and the vacuum field, respectively. The Hamiltonian for the atom is written as

$$H_A = \sum_{j=1,2,3,4} E_j |j\rangle\langle j| \,, \tag{3}$$

where E_j is the energy of the level j. The energy E_2 is taken as the reference and is set as zero. We define the atomic transition operator for the transition from the upper level $|j\rangle$ to the lower level $|k\rangle$ as the lowering operator $\sigma_{jk} = |k\rangle\langle j|$ and for the transition from the lower level $|k\rangle$ to the upper level $|j\rangle$ as the raising operator $\sigma^\dagger_{jk} = |j\rangle\langle k|$. The expression of the Hamiltonian H_A can be rewritten as

$$H_A = -\hbar\omega_{21}\sigma_{21}\sigma^\dagger_{21} + \hbar\omega_{32}\sigma^\dagger_{32}\sigma_{32} + \hbar\omega_{42}\sigma^\dagger_{42}\sigma_{42}\,, \tag{4}$$

where $\sigma_{21}\sigma^\dagger_{21} = |1\rangle\langle 1|$, $\sigma^\dagger_{32}\sigma_{32} = |3\rangle\langle 3|$, $\sigma^\dagger_{42}\sigma_{42} = |4\rangle\langle 4|$ and ω_{jk} denotes the respective atomic transition frequency. If a_1 and a_2 ($a^\dagger_1$ and $a^\dagger_2$) are assumed to be the annihilation (creation) operators for the single-mode driving fields $E(\omega_1)$ and $E(\omega_2)$ respectively, the Hamiltonian H_F can be expressed as

$$H_F = \hbar\omega_1 a^\dagger_1 a_1 + \hbar\omega_2 a^\dagger_2 a_2\,. \tag{5}$$

Similarly, the Hamiltonian H_V can be written as

$$H_V = \sum_k \hbar\omega_k a^\dagger_k a_k\,, \tag{6}$$

where a_k ($a^\dagger_k$) is the annihilation (creation) operator for the $k^{\rm th}$ vacuum mode with frequency ω_k. The time evolution of the atomic and field operators is determined by considering the operator equation of motion in the interaction picture. On restricting to the electric-dipole approximation, the Hamiltonian H' can be expressed in the interaction picture by using the rotating wave approximation (RWA) [37] as

$$H'_{\rm int} = \hbar[(g_1\sigma^\dagger_{42}a_1{\rm e}^{-{\rm i}\Delta_1 t} + H.c.) + (g_2\sigma^\dagger_{32}a_2{\rm e}^{-{\rm i}\Delta_2 t} + H.c.) + \sum_k (g_k\sigma^\dagger_{21}a_k{\rm e}^{-{\rm i}\Delta_k t} + H.c.)], \tag{7}$$

where the detuning terms are $\Delta_1 = \omega_1 - \omega_{42}$, $\Delta_2 = \omega_2 - \omega_{32}$ and $\Delta_k = \omega_k - \omega_{21}$. We define the state vector of the total system in the interaction picture at time t as

$$\begin{aligned} |\psi\rangle_{\rm int} \;\; = \;\; & \sum_k b_{1,k}|1, n_1, n_2\rangle|1_k\rangle + b_2|2, n_1, n_2\rangle|\{0\}\rangle \\ & + b_3|3, n_1, (n_2-1)\rangle|\{0\}\rangle + b_4|4, (n_1-1), n_2\rangle|\{0\}\rangle\,, \end{aligned} \tag{8}$$

where n_j is the number of photons in the single-mode fields, $|1_k\rangle$ represents the state with one photon in the $k^{\rm th}$ vacuum mode and $|\{0\}\rangle$ represents the absence of photon state. Without loss of generality, the coupling constants are taken to be real [37]. By substituting Eqs. (7) and (8) in the Schrödinger's equation

$${\rm i}\hbar\frac{\partial}{\partial t}|\psi\rangle_{\rm int} = H'_{\rm int}|\psi\rangle_{\rm int}\,, \tag{9}$$

we obtain the equations of motion for the probability amplitudes as follows

$$\dot{b}_{1,k} = -\mathrm{i}g_k \mathrm{e}^{\mathrm{i}\Delta_k t} b_2 \,, \tag{10}$$

$$\dot{b}_2 = -\mathrm{i}\sum_k g_k \mathrm{e}^{-\mathrm{i}\Delta_k t} b_{1,k} - \mathrm{i}g_2\sqrt{n_2}\mathrm{e}^{\mathrm{i}\Delta_2 t} b_3 - \mathrm{i}g_1\sqrt{n_1}\mathrm{e}^{\mathrm{i}\Delta_1 t} b_4 \,, \tag{11}$$

$$\dot{b}_3 = -\mathrm{i}g_2\sqrt{n_2}\mathrm{e}^{-\mathrm{i}\Delta_2 t} b_2 \,, \tag{12}$$

$$\dot{b}_4 = -\mathrm{i}g_1\sqrt{n_1}\mathrm{e}^{-\mathrm{i}\Delta_1 t} b_2 \,. \tag{13}$$

We assume $\Omega_1 = g_1\sqrt{n_1}$ and $\Omega_2 = g_2\sqrt{n_2}$. They can be treated as the equivalent Rabi frequencies of two coherent fields as obtained in the semiclassical picture. On using the initial condition $b_{1,k}(0) = 0$, we obtain from Eq. (10)

$$b_{1,k}(t) = -\mathrm{i}g_k \int_0^t \mathrm{e}^{\mathrm{i}\Delta_k t'} b_2(t')\mathrm{d}t'. \tag{14}$$

In Eq. (11), we replace $\sum_k$ by $\int_0^\infty \mathrm{d}\omega_k D(\omega_k)$ [37,38] and substitute $b_{1,k}(t)$ from Eq. (14). Here $D(\omega_k) = V\omega_k^2/(\pi^2 c^3)$, which represents the density of states per unit frequency range in the interval between ω_k and $\omega_k + \mathrm{d}\omega_k$ within the quantization volume V. We follow the well known Weisskopf-Wigner approach [37] to obtain

$$\dot{b}_2 = -\frac{\gamma_2}{2} b_2 - \mathrm{i}\Omega_2 \mathrm{e}^{\mathrm{i}\Delta_2 t} b_3 - \mathrm{i}\Omega_1 \mathrm{e}^{\mathrm{i}\Delta_1 t} b_4 \,. \tag{15}$$

The explicit time dependence lying in Eqs. (12), (13) and (15) can be removed by introducing the transformations $b_3 = c_3\ \mathrm{e}^{-\mathrm{i}\Delta_2 t}$ and $b_4 = c_4\ \mathrm{e}^{-\mathrm{i}\Delta_1 t}$ [39]. Then Eqs. (12), (13) and (15) can be written as follows

$$\dot{b}_2 = -\frac{\gamma_2}{2} b_2 - \mathrm{i}\Omega_2 c_3 - \mathrm{i}\Omega_1 c_4 \,, \tag{16}$$

$$\dot{c}_3 = -\mathrm{i}\Omega_2 b_2 + \mathrm{i}\Delta_2 c_3 \,, \tag{17}$$

$$\dot{c}_4 = -\mathrm{i}\Omega_1 b_2 + \mathrm{i}\Delta_1 c_4 \,. \tag{18}$$

In order to find nonvanishing population in the upper states, the determinant of the coefficient-matrix for the variables b_2, c_3 and c_4 in the set of Eqs. (16) – (18) must be equal to zero, i.e.

$$\frac{\gamma_2}{2}\Delta_1\Delta_2 + \mathrm{i}(\Omega_1^2\Delta_2 + \Omega_2^2\Delta_1) = 0 \,. \tag{19}$$

Thus the resulting condition for population trapping [1] is satisfied when the real and imaginary parts of Eq. (19) are simultaneously zero for $\Delta_1 = \Delta_2 = 0$.

2.1.1. Emission spectra

The steady-state expression for the probability amplitude $b_{1,k}$ can be obtained by changing the upper limit of integration in Eq. (14) into infinity [12, 39]

$$b_{1,k}(t \to \infty) = -\mathrm{i} g_k [b_2(s)]_{s=-\mathrm{i}\Delta_k}, \tag{20}$$

where $b_2(s) = \int\limits_0^\infty b_2(t)\mathrm{e}^{-st}\mathrm{d}t$; s is the Laplace space variable.

By solving Eqs. (16) – (18) in Laplace space, we evaluate

$$b_2(s) = \frac{(s-\mathrm{i}\Delta_1)(s-\mathrm{i}\Delta_2)b_2(0) - \mathrm{i}\Omega_2(s-\mathrm{i}\Delta_1)c_3(0) - \mathrm{i}\Omega_1(s-\mathrm{i}\Delta_2)c_4(0)}{(s+\gamma_2/2)(s-\mathrm{i}\Delta_1)(s-\mathrm{i}\Delta_2) + \Omega_2^2(s-\mathrm{i}\Delta_1) + \Omega_1^2(s-\mathrm{i}\Delta_2)}\,. \tag{21}$$

The spontaneous emission spectrum is the Fourier transform of the field-correlation function $\langle E^-(t+\tau)E^+(t)\rangle_{t\to\infty}$, and can be written as [12, 39]

$$S(\Delta_k) = \frac{\gamma_2}{2\pi g_k^2} |b_{1,k}(t\to\infty)|^2\,. \tag{22}$$

The spectrum $S(\Delta_k)$ as defined in the above equation can be obtained finally by using Eqs. (20) and (21) in the following form

$$S(\Delta_k) = \frac{\gamma_2}{2\pi} \left| \frac{b_2(0) + \dfrac{\Omega_2}{\Delta_k+\Delta_2}c_3(0) + \dfrac{\Omega_1}{\Delta_k+\Delta_1}c_4(0)}{\mathrm{i}\Delta_k - \dfrac{\gamma_2}{2} + \dfrac{\Omega_2^2}{\mathrm{i}(\Delta_k+\Delta_2)} + \dfrac{\Omega_1^2}{\mathrm{i}(\Delta_k+\Delta_1)}} \right|^2. \tag{23}$$

In the case of very weak coupling fields, the spectrum $S(\Delta_k)$ can be simplified by the following expression

$$S(\Delta_k) = \frac{\gamma_2}{2\pi} \left| \frac{b_2(0)}{\mathrm{i}\Delta_k - \gamma_2/2} \right|^2. \tag{24}$$

The spectrum in Eq. (22) represents a single Lorentzian profile around $\Delta_k = 0$.

From Eq. (23), it can be shown that the *complete quenching* of spontaneous emission is possible. In this context, $b_2(0)$ is taken to be zero. When $\Omega_1 = \Omega_2$, $\Delta_1 = \Delta_2$ and $c_3(0) = -c_4(0)$, $S(\Delta_k)$ is found to be zero for all values of Δ_k. For this purpose, the excited states $|3\rangle$ and $|4\rangle$ will have to be initially prepared in their coherent superposition state [33].

When $b_2(0)$ is taken to be nonzero, one can obtain *selective quenching* of emission for different values of Rabi frequencies and detuning. If we consider the situation for $c_j(0) \ll b_2(0)$, then two quenching points occur at the positions $\Delta_k = -\Delta_1$, $-\Delta_2$. In this case, the spectrum $S(\Delta_k)$ can be expressed as

$$S(\Delta_k) = \frac{\gamma_2}{2\pi} \left| \frac{(\Delta_k+\Delta_1)(\Delta_k+\Delta_2)b_2(0)}{(\Delta_k+\mathrm{i}\gamma_2/2)(\Delta_k+\Delta_1)(\Delta_k+\Delta_2) - \Omega_1^2(\Delta_k+\Delta_2) - \Omega_2^2(\Delta_k+\Delta_1)} \right|^2. \tag{25}$$

The quenching points are surrounded by three spectral-peaks, what can be envisaged from the analysis of imaginary part of the denominator in the right-hand side of Eq. (25). For $|\Delta_1| = |\Delta_2| = \Delta$, the quenching points coincide at $\Delta_k = -\Delta$ and the three-peak spectrum reduces into two-peak spectrum.

At the condition of population trapping ($\Delta_1 = \Delta_2 = 0$) as suggested by Eq. (19), it is straightforward from Eq. (23) to derive the spontaneous emission spectrum

$$S(\Delta_k) = \frac{\gamma_2}{2\pi} \left| \frac{\Delta_k + \Omega_2 \dfrac{c_3(0)}{b_2(0)} + \Omega_1 \dfrac{c_4(0)}{b_2(0)}}{\Delta_k(\Delta_k + \dfrac{\gamma_2}{2}) - \Omega_1^2 - \Omega_2^2} \right|^2 b_2^2(0)\,. \tag{26}$$

So the emission does not vanish at $\Delta_k = 0$ unless $\Omega_2 c_3(0)/b_2(0) + \Omega_1 c_4(0)/b_2(0) = 0$. We mention that for high values of Rabi frequencies, the absolute suppression of emission is possible at $\Delta_k = 0$ depending on the Rabi-splitting effect.

By setting the values of Rabi frequencies as $\Omega_1 = \Omega_2 = 10\gamma_2$, we obtain all spectral features which are accordingly presented in Fig. 2 by the curves (a) ($\Delta_1 = \Delta_2 = 10\gamma_2$) for $b_2(0) = 0$, $c_3(0) = -c_4(0) = 0.5$, and (b) ($\Delta_1 = -\Delta_2 = 10\gamma_2$), (c) ($\Delta_1 = \Delta_2 = 0$), (d) ($\Delta_1 = \Delta_2 = 10\gamma_2$) for $b_2(0) = 1$, $c_3(0) = c_4(0) = 0$.

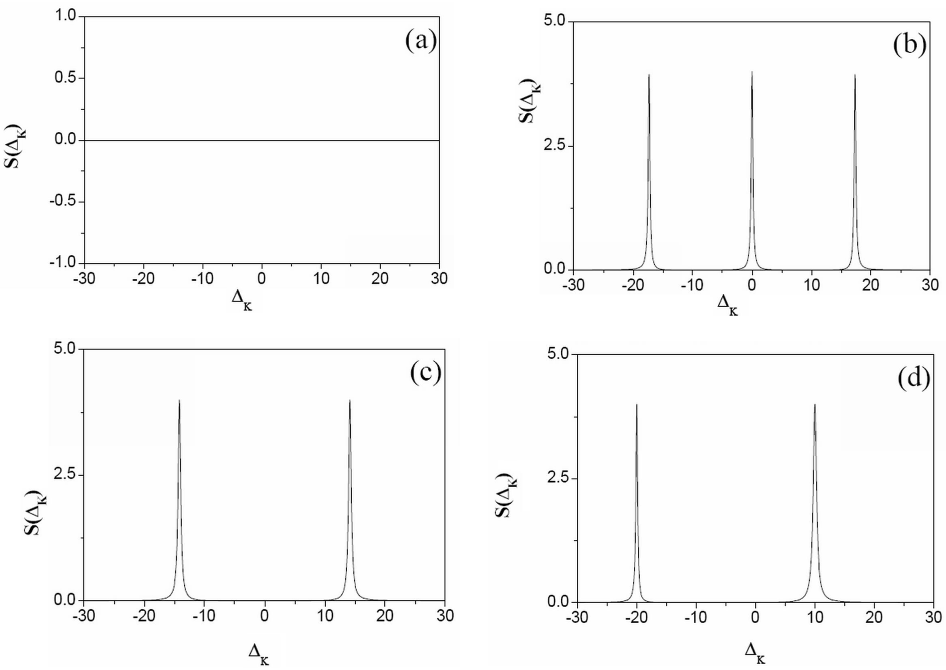

Fig. 2. Resonant and non-resonant evolution of spontaneous emission specta in the ideal bare-state model for $R_1 = R_2 = 10$. Other parameters are: (a) $\Delta_1 = \Delta_2 = 10$, $b_2(0) = 0$ and $c_3(0) = -c_4(0) = 0.5$, (b) $\Delta_1 = -\Delta_2 = 10$, $b_2(0) = 1$ and $c_3(0) = c_4(0) = 0$, (c) $\Delta_1 = \Delta_2 = 0$, $b_2(0) = 1$ and $c_3(0) = c_4(0) = 0$, (d) $\Delta_1 = \Delta_2 = 10$, $b_2(0) = 1$ and $c_3(0) = c_4(0) = 0$. All rates are in units of γ_2.

2.2. Dressed-state interpretation

Origin of the spectral components can be analyzed in the dressed-state picture (Fig. 1b) of both coupling fields operating in the excited states of the system. In this respect, we consider the reversible dynamics represented by Eqs. (16) – (18) of motion of the probability amplitudes b_2, c_3 and c_4. Thus, the characteristic equation of the interaction Hamiltonian-matrix can be represented as,

$$\xi^3 + (\Delta_1 + \Delta_2)\xi^2 + [\Delta_1\Delta_2 - (\Omega_1^2 + \Omega_2^2)]\xi - (\Omega_1^2\Delta_2 + \Omega_2^2\Delta_1) = 0\,. \qquad (27)$$

For different combinations of the driving fields with typical values of the Rabi frequencies and detuning parameters, the formation of dressed states corresponding to the eigenvalues ξ_i will be different. In the following, we discuss the dynamical evolution of spectra as presented in Fig. 2 in different occasions.

At the condition of population trapping for $\Delta_1 = \Delta_2 = 0$, we obtain the eigenvalues $\xi_0 = 0$, $\xi_\pm = \pm\sqrt{\Omega_1^2 + \Omega_2^2}$. The energy levels $|2\rangle$, $|3\rangle$ and $|4\rangle$ in the bare-state model can be replaced by the new eigenstates $|+\rangle$, $|0\rangle$ and $|-\rangle$ whose probability amplitudes are given as

$$b_+ = \frac{1}{\sqrt{2}}b_2 + \frac{1}{\sqrt{2}}\cos\theta\ c_3 + \frac{1}{\sqrt{2}}\sin\theta\ c_4\,, \qquad (28)$$

$$b_0 = -\sin\theta c_3 + \cos\theta\ c_4\,, \qquad (29)$$

$$b_- = \frac{1}{\sqrt{2}}b_2 - \frac{1}{\sqrt{2}}\cos\theta\ c_3 - \frac{1}{\sqrt{2}}\sin\theta\ c_4\,, \qquad (30)$$

where $\sin\theta = \dfrac{\Omega_1}{\sqrt{\Omega_1^2+\Omega_2^2}}$, $\cos\theta = \dfrac{\Omega_2}{\sqrt{\Omega_1^2+\Omega_2^2}}$. We note that three bare-states $|2\rangle$, $|3\rangle$ and $|4\rangle$ individually contribute to the formation of the states $|\pm\rangle$, whereas the antisymmetric superposition of states $|3\rangle$ and $|4\rangle$ gives rise to the state $|0\rangle$ which is decoupled from the state $|2\rangle$. The atom initially in the state $|2\rangle$ gives rise to the coherent transfer of population into the dressed states $|3\rangle$ and $|4\rangle$.

By using Eqs. (28) – (30), after some algebraic calculations, Eqs. (16) – (18) can be replaced by

$$\dot{b}_+ = -(\frac{\gamma_+}{2} + \mathrm{i}\Omega_+)b_+ - \frac{\sqrt{\gamma_+\gamma_-}}{2}b_- + \mathrm{i}\Omega_0 b_0\,, \qquad (31)$$

$$\dot{b}_0 = \mathrm{i}\Omega_0 b_+ + \mathrm{i}\Omega_0 b_-\,, \qquad (32)$$

$$\dot{b}_- = -(\frac{\gamma_-}{2} - \mathrm{i}\Omega_-)b_- - \frac{\sqrt{\gamma_+\gamma_-}}{2}b_+ + \mathrm{i}\Omega_0 b_0\,, \qquad (33)$$

where $\gamma_+ = \gamma_- = \gamma_2/2$, $\Omega_+ = \Omega_- = \Omega_2\cos\theta + \Omega_1\sin\theta$ and $\Omega_0 = \Omega_2\sin\theta - \Omega_1\cos\theta$. As the decay rates of the dressed-states $|\pm\rangle$ are equal, the spectrum will contain two symmetric peaks (Fig. 2c), one at each position of the dressed states. We note that the dressed states $|\pm\rangle$ can decay at a slower rate $(\gamma_2/2)$ in comparison to the decay rate γ_2 of the bare-state $|2\rangle$. Two dressed levels $|\pm\rangle$ can interact with each other via their spontaneous decay channels as can be interpreted by the presence of the term $\sqrt{\gamma_+\gamma_-}/2$ in Eqs. (31) and (33).

When the values of the detuning parameters Δ_1 and Δ_2 are equal and opposite, we can impose the following condition on Eq. (27)

$$\left(\frac{\Omega_1}{\Omega_2}\right)^2 = -\frac{\Delta_1}{\Delta_2}\,. \tag{34}$$

For further simplification we assume $|\Delta_1| = |\Delta_2| = \Omega_1 = \Omega_2 = \eta$ (say). Then the eigenvalues are given as $\xi_0 = 0$, $\xi_\pm = \pm\sqrt{3}\eta$. Correspondingly, the probability amplitudes of the dressed states can be expressed as

$$\begin{aligned} b_+ &= -\frac{2}{\sqrt{12}}b_2 - \frac{1+\sqrt{3}}{\sqrt{12}}c_3 + \frac{1-\sqrt{3}}{\sqrt{12}}c_4\,, && (35)\\ b_0 &= \frac{1}{\sqrt{3}}b_2 - \frac{1}{\sqrt{3}}c_3 + \frac{1}{\sqrt{3}}c_4\,, && (36)\\ b_- &= -\frac{2}{\sqrt{12}}b_2 - \frac{1-\sqrt{3}}{\sqrt{12}}c_3 + \frac{1+\sqrt{3}}{\sqrt{12}}c_4\,. && (37)\end{aligned}$$

In the present case, the dynamical Eqs. (31) – (33) take the following forms

$$\dot{b}_+ = -\left[\frac{\gamma_+}{2}+\mathrm{i}\eta\left(\frac{12+\sqrt{6}}{3\sqrt{2}}\right)\right]b_+ + \frac{\sqrt{\gamma_+\gamma_0}}{2}b_0 - \left[\frac{\sqrt{\gamma_+\gamma_-}}{2}-\mathrm{i}\eta\left(\frac{6-\sqrt{6}}{3\sqrt{2}}\right)\right]b_-\,, \tag{38}$$

$$\dot{b}_0 = -\frac{\gamma_0}{2}b_0 + \frac{\sqrt{\gamma_+\gamma_0}}{2}b_+ + \frac{\sqrt{\gamma_-\gamma_0}}{2}b_-\,, \tag{39}$$

$$\dot{b}_- = -\left[\frac{\gamma_-}{2}-\mathrm{i}\eta\left(\frac{12+\sqrt{6}}{3\sqrt{2}}\right)\right]b_- + \frac{\sqrt{\gamma_-\gamma_0}}{2}b_0 - \left[\frac{\sqrt{\gamma_+\gamma_-}}{2}+\mathrm{i}\eta\left(\frac{6-\sqrt{6}}{3\sqrt{2}}\right)\right]b_+\,, \tag{40}$$

where $\gamma_+ = \gamma_0 = \gamma_- = \gamma_2/3$. The appearance of the interference terms with positive or negative signs in Eqs. (38) – (40) suggests that the effect of decay-interference on the central peak arising from the dressed state $|0\rangle$ is constructive. Thus the profiles of three peaks (Fig. 2b) in the emission spectrum can be asymmetric for a particular set of values of Rabi frequencies and detunings of the coupling fields.

We also consider the situation when Δ_1, Δ_2, Ω_1 and Ω_2 are of equal magnitudes and Δ_1, Δ_2 are of the same sign. Then we should have the following relationship

$$\Omega_1^2\Delta_2 + \Omega_2^2\Delta_1 = -(\Delta_1+\Delta_2)[\Delta_1\Delta_2 - (\Omega_1^2+\Omega_2^2)]. \tag{41}$$

Making use of the above equation, we solve the Eq. (27) to find out the eigenvalues for $|\Delta_1| = |\Delta_2| = \Omega_1 = \Omega_2 = \chi$ (say). Now we obtain the eigenvalues $\xi_+ = \chi$,

$\xi_0 = -\chi$ and $\xi_- = -2\chi$. The probability amplitudes of the corresponding eigenvectors are given as

$$b_+ = \frac{2}{\sqrt{6}}b_2 + \frac{1}{\sqrt{6}}c_3 + \frac{1}{\sqrt{6}}c_4\,, \tag{42}$$

$$b_0 = \frac{1}{\sqrt{2}}c_3 - \frac{1}{\sqrt{2}}c_4\,, \tag{43}$$

$$b_- = \frac{1}{\sqrt{3}}b_2 - \frac{1}{\sqrt{3}}c_3 - \frac{1}{\sqrt{3}}c_4\,. \tag{44}$$

The state $|0\rangle$ results from coherent superposition of two bare states $|3\rangle$ and $|4\rangle$, and is decoupled from the other state $|2\rangle$. Hence, the dressed state $|0\rangle$ remains unpopulated. The equations of motion for the probability amplitudes of the dressed states can be given as

$$\dot{b}_+ = -(\gamma_+/2 \ + \mathrm{i}\chi)b_+ - \gamma_{\mathrm{int}}b_-\,, \tag{45}$$

$$\dot{b}_0 = \mathrm{i}\chi b_0\,, \tag{46}$$

$$\dot{b}_- = -(\gamma_-/2 \ - \mathrm{i}2\chi)b_- - \gamma_{\mathrm{int}}b_+\,, \tag{47}$$

where $\gamma_+ = 2\gamma_2/3$, $\gamma_- = \gamma_2/3$ and $\gamma_{\mathrm{int}} = \gamma_2/(3\sqrt{2})$. The decaying nature of the dressed states leads to an asymmetric two-peak spectrum (Fig. 2d).

We note that the spectral features exhibited in Figs. 2a-d are obtained in the present model without incorporating the decays from the upper excited states. Such a model can be realized when, instead of the one-photon process, the transitions from the state $|2\rangle$ to the upper excited states are governed by the two-photon transition processes [40, 41]. In this situation, the Rabi frequencies Ω_1 and Ω_2 can be regarded to be the effective two-photon Rabi frequencies [40, 41], i.e. $\Omega_i = \sum_k \Omega_{2k}\Omega_{kj}\left(\frac{1}{\omega_k - \omega_a} + \frac{1}{\omega_k - \omega_b}\right)$ for $i = 1, 2$ and $j = 3, 4$; k denotes the intermediate states, ω_a and ω_b are the frequencies of the absorbed two photons.

3. *Emission under dissipative environment*

For the non-decaying energy levels $|3\rangle$ and $|4\rangle$, we have already shown that if the Rabi frequencies and the detuning parameters of the coupling fields in the upper transitions follow a certain relationship, there will be a condition of population trapping in the upper states. The inclusion of decays from the upper energy levels $|3\rangle$ and $|4\rangle$ to their next lower level will, in general, disrupt the ideal condition of population trapping. If we consider the purely dissipative environment of the atom, it needs to incorporate the effect of natural de-excitation of the upper states $|3\rangle$ and $|4\rangle$ in their respective one-photon transition channels. We also include the effect of application of an incoherent field (a broadband source) in the lower transition

$|2\rangle \leftrightarrow |1\rangle$. The incoherent pumping is considered to be in both directions [28]; the rate of population transfer from level $|1\rangle$ to $|2\rangle$ and back is denoted by Λ. To obtain the quantitative results in the present model, it is convenient to describe the system by standard density-matrix formalism, and the spontaneous emission spectrum can be obtained with the use of the quantum regression theorem [37].

3.1. Theoretical formulation

The coupling fields acting in the upper transitions are defined classically, i.e. $E(\omega_j, t) = (E_j/2)\mathrm{e}^{\mathrm{i}\omega_j t} + c.c.$ $(j = 1, 2)$. In the present formulation, we have ignored the non-radiative transitions among the atomic states due to interatomic collisions. The dynamical behaviour of the system under consideration can be represented by the time evolution of the density-matrix operator [19]

$$\frac{\partial \rho'}{\partial t} = \left(\frac{\partial \rho'}{\partial t}\right)_{\text{reversible}} + \left(\frac{\partial \rho'}{\partial t}\right)_{\text{spon.damping}} + \left(\frac{\partial \rho'}{\partial t}\right)_{\text{inco.pumping}}, \tag{48}$$

where the reversible part represents the interaction between coherent fields and medium and can be given as

$$\left(\frac{\partial \rho'}{\partial t}\right)_{\text{reversible}} = -\frac{\mathrm{i}}{\hbar}[H', \rho']. \tag{49}$$

The irreversible dynamics of the system can be obtained by following the generalized system-reservoir interaction for the dissipative process [39]. We can derive the expression for the rate of change of density operator relating to the spontaneous relaxation as given below

$$\begin{aligned}\left(\frac{\partial \rho'}{\partial t}\right)_{\text{spon.damping}} &= -\frac{\gamma_2}{2}[\{|2\rangle\langle 2|, \rho'\} - 2|1\rangle\langle 2|\rho'|2\rangle\langle 1|] \\ &\quad - \sum_{j=3,4} \frac{\gamma_j}{2}[\{|j\rangle\langle j|, \rho'\} - 2|2\rangle\langle j|\rho'|j\rangle\langle 2|]\,. \end{aligned}\tag{50}$$

The rate of change of density operator corresponding to the incoherent pumping process can be represented as

$$\left(\frac{\partial \rho'}{\partial t}\right)_{\text{inco.pumping}} = -\frac{\Lambda}{2} \sum_{j=1,2} [\{|j\rangle\langle j|, \rho'\} - \sum_{k(\neq j)=1,2} 2|j\rangle\langle k|\rho'|k\rangle\langle j|]\,. \tag{51}$$

Under the dipole-approximation, on using the rotating wave approximation (RWA), the perturbation Hamiltonian H' in the interaction picture is represented in the time-invariant form [39]

$$H'_{\text{int}} = -\hbar[\Delta_2|3\rangle\langle 3| + \Delta_1|4\rangle\langle 4| + (R_2|2\rangle\langle 3| + R_1|2\rangle\langle 4| + H.c.)]\,, \tag{52}$$

where the detunings of the fields from their respective resonances are written as $\Delta_1 = \omega_1 - \omega_{42}$ and $\Delta_2 = \omega_2 - \omega_{32}$, and the coupling of the atom with the coherent fields are denoted by the Rabi frequencies $R_1 = \bar{\mu}_{24}.\bar{E}_1/(2\hbar)$ and $R_2 = \bar{\mu}_{23}.\bar{E}_2/(2\hbar)$, respectively. By introducing the transformations: $R_j = |R_j|\ \mathrm{e}^{\mathrm{i}\theta_j}(j = 1,2)$, $\rho'_{kk} = \rho_{kk}(k = 1,2,3,4)$, $\rho'_{12} = \rho_{12}$, $\rho'_{13} = \rho_{13}\mathrm{e}^{-\mathrm{i}\theta_2}$, $\rho'_{14} = \rho_{14}\mathrm{e}^{-\mathrm{i}\theta_1}$, $\rho'_{23} = \rho_{23}\mathrm{e}^{-\mathrm{i}\theta_2}$, $\rho'_{24} = \rho_{24}\mathrm{e}^{-\mathrm{i}\theta_1}$ and $\rho'_{34} = \rho_{34}\mathrm{e}^{\mathrm{i}(\theta_2-\theta_1)}$; $\theta_j(j = 1,2)$ are the phase parameters, the set of equations of the required elements of the atomic density matrix are obtained as follows

$$\dot{\rho}_{11} = -\Lambda\rho_{11} + (\Lambda + \gamma_2)\rho_{22}\,, \tag{53}$$

$$\dot{\rho}_{22} = \Lambda\rho_{11} - (\Lambda+\gamma_2)\rho_{22} + \gamma_3\rho_{33} + \gamma_4\rho_{44} + \mathrm{i}|R_1|(\rho_{42} - \rho_{24}) + \mathrm{i}|R_2|(\rho_{32} - \rho_{23}), \tag{54}$$

$$\dot{\rho}_{33} = -\gamma_3\rho_{33} + \mathrm{i}|R_2|(\rho_{23} - \rho_{32})\,, \tag{55}$$

$$\dot{\rho}_{44} = -\gamma_4\rho_{44} + \mathrm{i}|R_1|(\rho_{24} - \rho_{42})\,, \tag{56}$$

$$\dot{\rho}_{12} = -\Gamma_{12}\rho_{12} - \mathrm{i}|R_1|\rho_{14} - \mathrm{i}|R_2|\rho_{13}\,, \tag{57}$$

$$\dot{\rho}_{13} = -(\Gamma_{13} + \mathrm{i}\Delta_2)\rho_{13} - \mathrm{i}|R_2|\rho_{12}\,, \tag{58}$$

$$\dot{\rho}_{14} = -(\Gamma_{14} + \mathrm{i}\Delta_1)\rho_{14} - \mathrm{i}|R_1|\rho_{12}\,, \tag{59}$$

$$\dot{\rho}_{23} = -(\Gamma_{23} + \mathrm{i}\Delta_2)\rho_{23} + \mathrm{i}|R_1|\rho_{43} + \mathrm{i}|R_2|(\rho_{33} - \rho_{22})\,, \tag{60}$$

$$\dot{\rho}_{24} = -(\Gamma_{24} + \mathrm{i}\Delta_1)\rho_{24} + \mathrm{i}|R_1|(\rho_{44} - \rho_{22}) + \mathrm{i}|R_2|\rho_{34}\,, \tag{61}$$

$$\dot{\rho}_{34} = -(\Gamma_{34} + \mathrm{i}(\Delta_1 - \Delta_2))\rho_{34} - \mathrm{i}|R_1|\rho_{32} + \mathrm{i}|R_2|\rho_{24}\,, \tag{62}$$

where $\Gamma_{12} = \Lambda + \gamma_2/2$, $\Gamma_{13} = (\Lambda + \gamma_3)/2$, $\Gamma_{14} = (\Lambda + \gamma_4)/2$, $\Gamma_{23} = (\Lambda + \gamma_2 + \gamma_3)/2$, $\Gamma_{24} = (\Lambda + \gamma_2 + \gamma_4)/2$ and $\Gamma_{34} = (\gamma_3 + \gamma_4)/2$.

3.1.1. **Emission spectra**

The spectrum of spontaneous emission on the transition $|2\rangle \leftrightarrow |1\rangle$ can be shown to be proportional to the function [42]

$$S(\Delta_k) = \int_0^\infty \mathrm{d}\tau\ \mathrm{e}^{-\mathrm{i}\Delta_k\tau} f(\tau) + c.c.\,, \tag{63}$$

where the function $f(\tau)$ is defined in terms of the two-time correlation function as

$$f(\tau) \equiv \langle\sigma^\dagger_{21}(t+\tau)\sigma_{21}(t)\rangle = \langle\sigma^\dagger_{21}(\tau)\sigma_{21}(0)\rangle. \tag{64}$$

In general, for the transition from the lower level $|k\rangle$ to the upper level $|j\rangle$ (as mentioned in Section 2), we have the time averaged dipole-transition operators: $\langle\sigma^\dagger_{jk}(0)\rangle = \rho_{kj}(0)$ and $\langle\sigma_{jk}(0)\rangle = \rho_{jk}(0)$, where $\rho_{kj}(0)$ (or $\rho_{jk}(0)$) is determined by the steady state value [42]. We use the Hermicity relation ($f(-\tau) = f^*(\tau)$) for the correlation function as introduced in Eq. (63). According to the rule of Laplace transformation, the steady state power spectrum of the fluorescence field [42] in the transition $|2\rangle \leftrightarrow |1\rangle$ can be determined by the following expression

$$S(\Delta_k) = 2\mathrm{Re}[\langle\sigma_{21}^{\dagger}(\tau)\sigma_{21}(0)\rangle]_{\tau=-\mathrm{i}\Delta_k}. \tag{65}$$

By solving the density matrix Eqs. (57) – (59) in Laplace space, we find out the correlation function on the basis of the quantum regression theorem. Thus the correlation function as defined in Eq. (64) can be expressed as

$$\begin{aligned}\langle\sigma_{21}^{\dagger}(\tau)\sigma_{21}(0)\rangle &= \frac{M_1\langle\sigma_{22}(0)\rangle - M_2\langle\sigma_{32}^{\dagger}(0)\rangle - M_3\langle\sigma_{42}^{\dagger}(0)\rangle}{M}\\ &= \frac{M_1\rho_{22}(0) - M_2\rho_{23}(0) - M_3\rho_{24}(0)}{M},\end{aligned} \tag{66}$$

where

$$\begin{aligned}M &= |R_1|^2(s+\Gamma_{13}+\mathrm{i}\Delta_2)+|R_2|^2(s+\Gamma_{14}+\mathrm{i}\Delta_1)+(s+\Gamma_{12})(s+\Gamma_{13}+\mathrm{i}\Delta_2)(s+\Gamma_{14}+\mathrm{i}\Delta_1),\\ M_1 &= (s+\Gamma_{13}+i\Delta_2)(s+\Gamma_{14}+i\Delta_1),\\ M_2 &= i|R_2|^2(s+\Gamma_{14}+i\Delta_1),\\ M_3 &= i|R_1|^2(s+\Gamma_{13}+i\Delta_2).\end{aligned} \tag{67}$$

The values of $\rho_{22}(0)$, $\rho_{23}(0)$ and $\rho_{24}(0)$ are determined by solving the density matrix equations in the steady state.

4. *Results and discussion*

In this section, we discuss the numerical results based on the spontaneous emission spectrum $S(\Delta_k)$ given in Eq. (65). All the rate-parameters used in the calculation are scaled by the decay rate γ_2. We assume $\gamma_2 = \gamma$. Other decay rates are chosen as $\gamma_3 = \gamma_4 = \gamma$.

At the two-photon Raman resonance ($\Delta_1 = \Delta_2 = 0$) condition, we have plotted the curves a ($\Lambda = 0.1\gamma$, $R_1 = R_2 = 6\gamma$), b ($\Lambda = \gamma$, $R_1 = R_2 = 6\gamma$) and c ($\Lambda = \gamma$, $R_1 = R_2 = 10\gamma$) in Fig. 3a. Two peaks having separation $2\sqrt{R_1^2 + R_2^2}$ result in the spectrum due to the strong two-photon coupling between the excited states $|3\rangle$ and $|4\rangle$. Dark feature is still present between two peaks of the spectrum represented by the curve a of Fig. 3a. With the increase of the incoherent pumping rate, peak height increases along with the increase in the broadening of the spectral peak as shown by the curve b of Fig. 3a. As a result of broadening, dark feature tends to disappear at the middle of the spectrum. For large values of Rabi frequencies, Rabi splitting effect dominates in the spectrum and the emission almost vanishes in the middle as shown by the curve c of Fig. 3a. We mention that, in the present dynamic

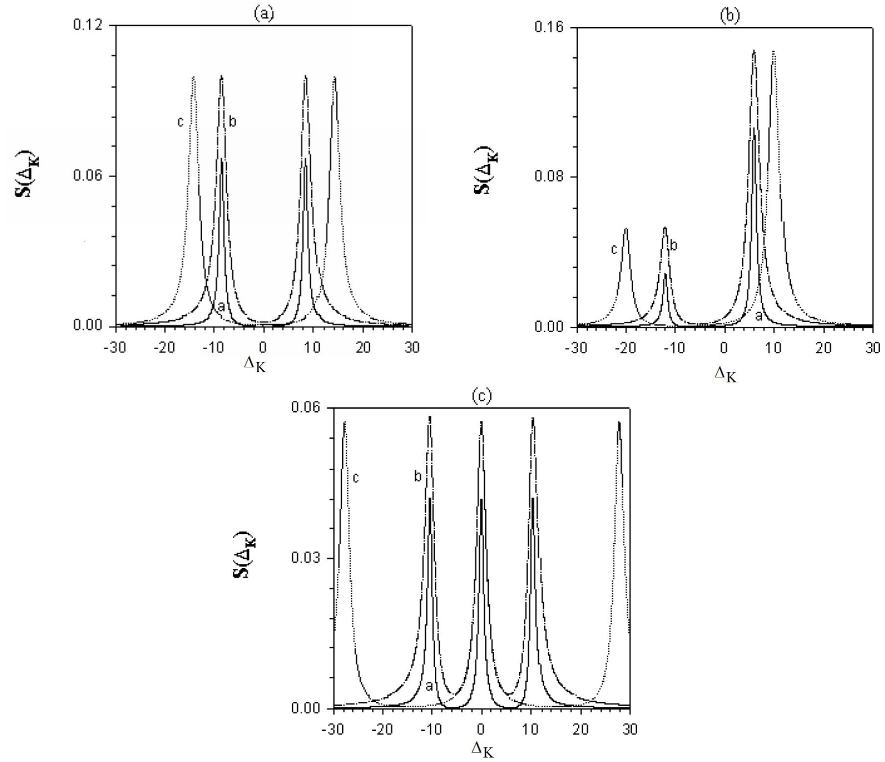

Fig. 3. Resonant and non-resonant evolution of spontaneous emission spectra in the present model under dissipative environment. For $R_1 = R_2 = R$ (say), we show (a) the curves a ($\Lambda = 0.1$, $R = 6$), b ($\Lambda = 1$, $R = 6$) and c ($\Lambda = 1$, $R = 10$) when $\Delta_1 = \Delta_2 = 0$; (b) the curves a ($\Lambda = 0.1$, $R = 6$), b ($\Lambda = 1$, $R = 6$) and c ($\Lambda = 1$, $R = 10$) when $\Delta_1 = \Delta_2 = R$, and (c) the curves a ($\Lambda = 0.1$, $R = 6$), b ($\Lambda = 1$, $R = 6$) and c ($\Lambda = 1$, $R = 16$) when $\Delta_1 = -\Delta_2 = R$. All rates are in units of γ_2.

condition, each of the two dressed states $|\pm\rangle$ generating the emission peaks decays with the rate

$$\Gamma_{+,-} \quad = \quad \frac{2(\gamma_2 + \Lambda) + \gamma_3 + \gamma_4}{4} = \gamma + \frac{\Lambda}{2}\,, \qquad (68)$$

The subnatural linewidths can be obtained for $(\gamma_3 + \gamma_4)/4 + \Lambda/2 < \gamma_2/2$ which is consistent with the decay rate mentioned in Section 2.2. We note that, unless $\gamma_3 + \gamma_4 < 2\gamma_2$, subnatural linewidth can not be obtained even if the incoherent pumping rate is zero.

If two coherent fields are tuned away from the condition of exact two-photon resonance ($\Delta_1 = \Delta_2 = \Delta$), two peaks occur with asymmetric heights in the spectrum as exhibited by curves a ($\Lambda = 0.1\gamma$, $R_1 = R_2 = 6\gamma$, $\Delta_1 = \Delta_2 = 6\gamma$), b ($\Lambda = \gamma$, $R_1 = R_2 = 6\gamma$, $\Delta_1 = \Delta_2 = 6\gamma$) and c ($\Lambda = \gamma$, $R_1 = R_2 = 10\gamma$, $\Delta_1 = \Delta_2 = 10\gamma$) in Fig. 3b. Quenching of emission, as represented by the curve d in Fig. 2, is still observable in the present condition. For the present condition of detunings and Rabi frequencies of the coherent fields, the decay rates of the dressed states can be expressed as

$$\Gamma_+ = \frac{12(\gamma_2+\Lambda)+\gamma_3+\gamma_4}{18} = \frac{7\gamma+6\Lambda}{9}\,,$$
$$\Gamma_- = \frac{3(\gamma_2+\Lambda)+\gamma_3+\gamma_4}{9} = \frac{5\gamma+3\Lambda}{9}\,. \tag{69}$$

The subnatural linewidths of the peaks corresponding to the dressed states $|+\rangle$ and $|-\rangle$ can be, respectively, obtained for $(\gamma_3+\gamma_4)/18 + 2\Lambda/3 \le 2\gamma_2/3$ and $(\gamma_3+\gamma_4)/9+\Lambda/3 \le \gamma_2/3$. The equality-sign holds for $\Lambda \ll (\gamma_3+\gamma_4)/12$. From Eq. (69), it is apparent that, for the values of $\Lambda < \gamma/3$ and $\Lambda < 4\gamma/3$, subnatural linewidth can be obtained for the emission peaks arising from the dressed states $|+\rangle$ and $|-\rangle$, respectively. We note that, for the value of $\Lambda = \gamma$, the width of the peak generated by the dressed state $|-\rangle$ is confined to subnatural regime.

For equal but opposite detuning of the coherent fields ($\Delta_1 = -\Delta_2 = \Delta$), we obtain in Fig. 3c the three-peak structure in the emission line shape due to the contribution of both dressed states $|\pm\rangle$ and $|0\rangle$. From the curves a ($\Lambda = 0.1\gamma$, $R_1 = R_2 = 6\gamma$, $\Delta_1 = -\Delta_2 = 6\gamma$), b ($\Lambda=\gamma$, $R_1 = R_2 = 6\gamma$, $\Delta_1 = -\Delta_2 = 6\gamma$) and c ($\Lambda = \gamma$, $R_1 = R_2 = 16\gamma$, $\Delta_1 = -\Delta_2 = 16\gamma$) in Fig. 3c, it is evident that at an appreciable value of the incoherent pumping rate, absolute suppression of emission is possible between successive peaks in the spectrum for sufficiently large values of Rabi frequencies of the external fields. In the given condition, three dressed states can decay with the following rates

$$\Gamma_0 = \frac{3(\gamma_2+\Lambda)+2(\gamma_3+\gamma_4)}{9} = \frac{7\gamma+3\Lambda}{9}\,,$$
$$\Gamma_+ = \Gamma_0 + \frac{\sqrt{3}(\gamma_3-\gamma_4)}{9} = \Gamma_0\,,$$
$$\Gamma_- = \Gamma_0 - \frac{\sqrt{3}(\gamma_3-\gamma_4)}{9} = \Gamma_0\,. \tag{70}$$

We note that, when the upper excited states decay with unequal rates, the larger is the difference between the values of the decay rates, the larger will be the the difference between the widths of two sideband peaks. The subnatural linewidths of the emission peaks arising from the dressed states $|0\rangle$, $|+\rangle$ and $|-\rangle$ can be respectively obtained for $\dfrac{2(\gamma_3+\gamma_4)}{9}+\dfrac{\Lambda}{3} \le \dfrac{\gamma_2}{3}$, $\dfrac{(2\sqrt{3}+1)\gamma_3+(2\sqrt{3}-1)\gamma_4}{9\sqrt{3}}+\dfrac{\Lambda}{3} \le \dfrac{\gamma_2}{3}$ and $\dfrac{(2\sqrt{3}-1)\gamma_3+(2\sqrt{3}+1)\gamma_4}{9\sqrt{3}}+\dfrac{\Lambda}{3} \le \dfrac{\gamma_2}{3}$. The equality-sign holds for $\Lambda \ll \dfrac{2(\gamma_3+\gamma_4)}{3}$. According to Eq. (70), the subnatural linewidth for each of the three emission peaks can be obtained for the values of $\Lambda < 2\gamma/3$. At the condition of non-resonant detuning of the coherent fields, it is interesting to note that in the absence of incoherent pumping rate in Eqs. (69) and (70), all spectral peaks will evolve in the subnatural regime.

Now we focus our attention to the generation of sideband peaks in the emission spectra for $\gamma_3 \neq \gamma_4$. Hence, we investigate the behaviour of spontaneous emission spectrum in Fig. 4 under the condition of non-resonant detuning ($\Delta_1 = -\Delta_2 = \Delta$) of the coherent fields with Rabi frequencies $R_1 = R_2 = R$ ($|R| \neq |\Delta|$). In Fig. 4a, we choose $R_1 = R_2 = 7\gamma$, $\Delta_1 = -\Delta_2 = 5\gamma$, $\gamma_4 = \gamma$ and $\Lambda = 0.1\gamma$ to plot the curves a ($\gamma_3 = \gamma$), b ($\gamma_3 = 10\gamma$), c ($\gamma_3 = 15\gamma$), d ($\gamma_3 = 18.5\gamma$) and e ($\gamma_3 = 22\gamma$). In the curve a ($\gamma_3 = \gamma_4$), almost at the positions $\Delta_k = \pm\sqrt{3}\eta$ ($\eta = |R|$), two enhanced sideband peaks occur with a less intense peak at their middle. With the increase in the value of γ_3, in the curves b-e, we observe that the middle and the right sideband peaks approach each other, and eventually merge at a point which is situated closely to their mid-position. This phenomenon occurs due to the constructive influence of multiple decay-interference of the dressed decay rates. The effect of this phenomenon increases with the increasing difference between the decay rates. Thus, as a result of quantum interference, along with the left sideband peak, a new peak occurs in the spectrum at the cost of other two residual peaks. For $R_1 = R_2 = 10\gamma$ and $\Lambda = 0.1\gamma$, Fig. 4b showns the curves a ($\gamma_3 = 10\gamma$, $\gamma_4 = \gamma$ and $\Delta_1 = -\Delta_2 = 9\gamma$), b ($\gamma_3 = 10\gamma$, $\gamma_4 = \gamma$ and $-\Delta_1 = \Delta_2 = 9\gamma$), c ($\gamma_3 = 10\gamma$, $\gamma_4 = \gamma$, $\Delta_1 = -\Delta_2 = 18\gamma$) and d ($\gamma_3 = \gamma$, $\gamma_4 = 10\gamma$, $\Delta_1 = -\Delta_2 = 18\gamma$). Curve a represents simultaneous enhancement of the left sideband peak and the suppression of the right sideband peak. If the detuning parameters are reversed, the nature of the curve a reverses its character as shown in curve b plotted for the same values of the decay rates. Without any change in the detuning condition, similar variation in the peak-distribution within the line shape is obtained when we reverse the values of γ_3 and γ_4 as clearly depicted by the curves c and d in Fig. 4b.

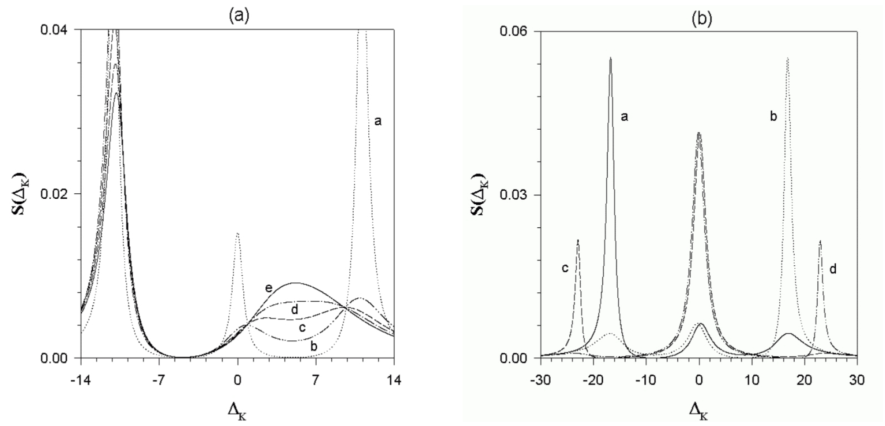

Fig. 4. Modification of emission line shape for unequal decay rates of the excited states $|3\rangle$ and $|4\rangle$. For $\gamma_4 = 1$, $\Lambda = 0.1$, $R_1 = R_2 = 7$ and $\Delta_1 = -\Delta_2 = 5$, we show in (a) the curves a ($\gamma_3 = 1$), b ($\gamma_3 = 10$), c ($\gamma_3 = 15$), d ($\gamma_3 = 18.5$) and e ($\gamma_3 = 22$). For $\Lambda = 0.1$ and $R_1 = R_2 = 10$, we show in (b) the curves a ($\gamma_3 = 10$, $\gamma_4 = 1$, $\Delta_1 = -\Delta_2 = 9$), b ($\gamma_3 = 10$, $\gamma_4 = 1$, $-\Delta_1 = \Delta_2 = 9$), c ($\gamma_3 = 10$, $\gamma_4 = 1$, $\Delta_1 = -\Delta_2 = 18$) and d ($\gamma_3 = 1$, $\gamma_4 = 10$, $\Delta_1 = -\Delta_2 = 18$). All rates are in units of γ_2.

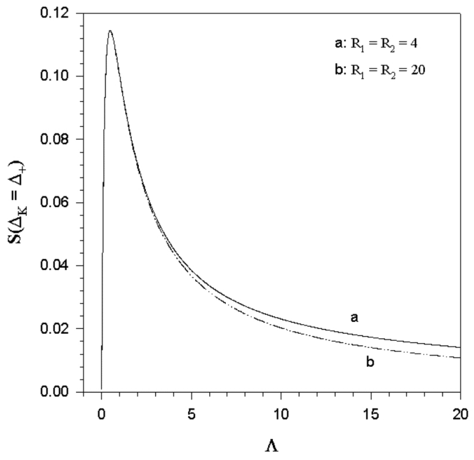

Fig. 5. Dependence of the line intensity on the incoherent pumping rate under the condition of resonant detuning of the fields. In the figure $\Delta_+ = \sqrt{R_1^2 + R_2^2}$. *All rates are in units of* γ_2.

To study the effect of incoherent pumping on the intensity of the peak, at the condition of resonant detuning of the coherent fields, we plotted two curves (a and b) in Fig. 5. It is found that, for higher values of Rabi frequencies, after attaining the maximum peak height, it decreases little more rapidly at larger values of Λ.

We end this section by presenting the following discussion. In our choice of decay rates, narrow non-resonant peaks could be observed in the emission spectra if the 'direct-pumping' scheme is replaced by an 'indirect-pumping' scheme. In order to avoid the 'direct-pumping' mechanism on experimentation, one could consider the two-photon excitation mechanism to populate an excited state $|e\rangle$ which is located above the bare states $|3\rangle$ and $|4\rangle$. Then, depending on the natural de-excitation of population from the state $|e\rangle$ to the lower states $|3\rangle$ and $|4\rangle$, the steady state fluorescence from level $|2\rangle$ can be detected. In such an experimental arrangement, as the incoherent contribution of the direct pumping rate Λ has no influence on the occurrence of coherent spectral features, for nearly equal values of the decay rates of the doublet $|3\rangle$ and $|4\rangle$, extremely narrow spectral components could be obtained in the emission spectrum as a result of quantum interference effect on the line wings.

5. *Static phase-variation effect*

In order to study the static phase-variation effect in our model, we take a similar Y-type system with a different field configuration. This model is chosen by considering closer separation of the excited states $|3\rangle$ and $|4\rangle$. In the present field configuration, two external fields of the same frequency can simultaneously interact with the excited doublet. Hence, in the prescribed model, one needs to redefine the

Rabi frequencies as

$$\begin{aligned} R_1 &= \frac{\bar{\mu}_{24}.(\bar{E}_1 + \bar{E}_2)}{2\hbar} = G_1 + G_1', \\ R_2 &= \frac{\bar{\mu}_{23}.(\bar{E}_1 + \bar{E}_2)}{2\hbar} = G_2' + G_2 \,. \end{aligned} \tag{71}$$

We choose, $G_1 = G_2 = G$ and $G_1' = G_2' = G'$ which lead to

$$|R_1|^2 = |R_2|^2 = |G|^2 + |G'|^2 + 2|G||G'|\cos(\phi)\,, \tag{72}$$

where ϕ denotes the phase difference which arises due to the mutual orientation of polarizations of the field modes. Thus, we replace the terms $|R_1|^2$ and $|R_2|^2$ in Eq. (67) of the Section 3.1.1 by the Eq. (72). We note that the phase ϕ, as introduced by the field polarization, remains static to the temporal evolution of the atomic system during interaction with the external fields.

When $\phi = \pi$, $|R_1|^2 = |R_2|^2 = 0$. Numerical computation of the spectrum $S(\Delta_k)$ as defined in Eq. (65) represents a single peak as shown by curve a($G = G' = 2\gamma$, $\Delta_1 = -\Delta_2 = 4\gamma$, $\Lambda = 0.1\gamma$) in Fig. 6. For the same values of detunings and Rabi frequencies, three peaks will result in the emission spectrum when $\phi = 2\pi/3$. This behaviour is shown in curve b of Fig. 6. If we set the value of $\phi = 0$, for the same values of other parameters, curve c in Fig. 6 represents the absolute suppression of the middle peak and simultaneously enhanced sideband peaks. If we compare curve a ($\phi = \pi$) to the curve c ($\phi = 0$), the respective appearance and almost disappearance of the middle peak in the emission spectrum constitute the phase-dependent switching effect.

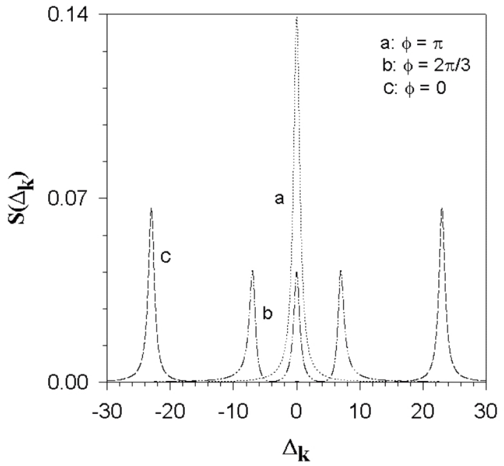

Fig. 6. Phase dependent evolution of spontaneous emission spectrum for $G = G' = 2$, $\Delta_1 = -\Delta_2 = 4$ and $\Lambda = 0.1$. All rates are in units of γ_2.

In Figs. 7a-c, we study the phase tuning effect on the emission spectrum for $G = G' = 2\gamma$ and $\Delta_1 = -\Delta_2 = 4\gamma$. There are two sets of curves, one is represented by the solid line for $\Lambda = 0.1\gamma$ and the other by the dotted line for $\Lambda = \gamma$. It is interesting to note here that, with the increase of the incoherent pumping rate, the narrow structures as developed in Figs. 7a,b can persist in the spectrum with less prominent behaviour of selective quenching of emission.

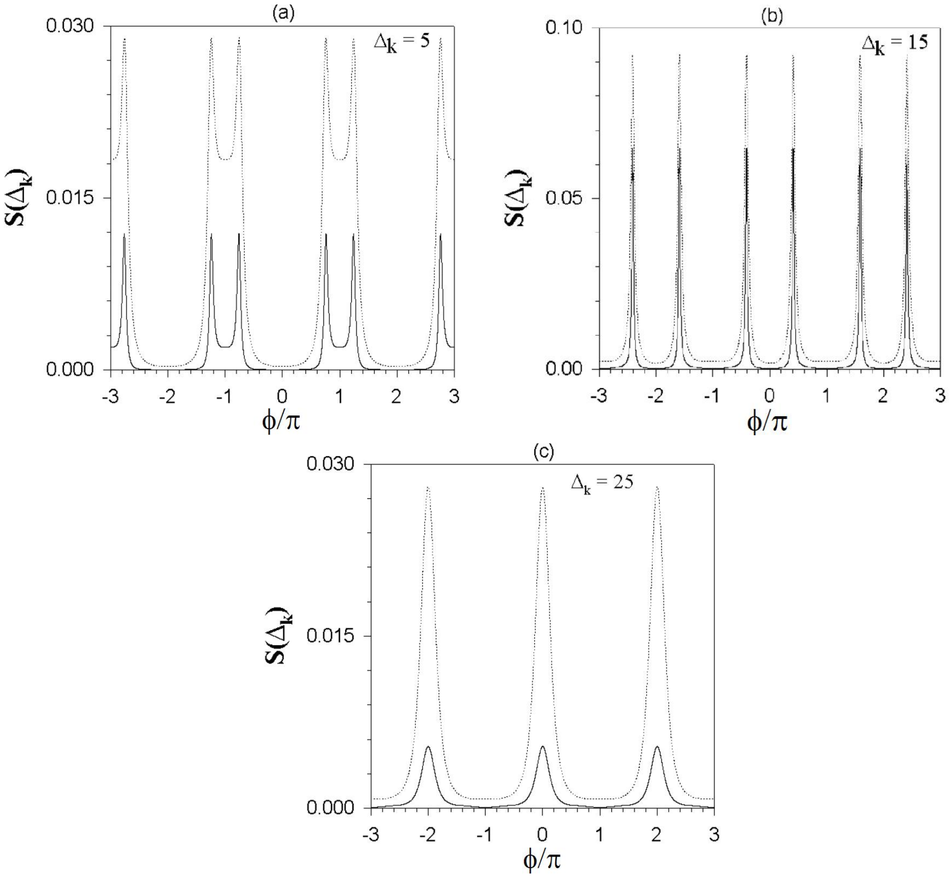

Fig. 7. Phase tuning effect on spontaneous emission spectrum for $G = G' = 2$ and $\Delta_1 = -\Delta_2 = 4$. In (a) – (c), the curves represented by the solid lines are for $\Lambda = 0.1$, while the curves represented by the dotted line are for $\Lambda = 1$. All rates are in units of γ_2.

6. Dynamic phase-variation effect

In contrast to the field configuration employed in Section 4, we can also consider that the external fields simultaneously interact with the upper excited states $|3\rangle$

and $|4\rangle$, and are of different frequencies and of the same static phase. Present field configuration in our Y-type model is shown in Fig. 8. On inclusion of frequency mismatch between the field components, a temporal phase fluctuation term along with the conventional detuning term evolves in the interaction Hamiltonian as given in section 2.1. Correspondingly, the rate Eqs. (16)−(18) in Section 2.1 of the probability amplitudes of the bare states $|2\rangle$, $|3\rangle$ and $|4\rangle$ contain the explicit time-dependent terms which are assumed to be rapidly varying in comparison to the slowly varying amplitudes of the excited states. On using this approximation based on the adiabatic evolution of the system under interaction, the time-independent interaction Hamiltonian of the system takes the following form

$$\begin{aligned} H'_{\rm int} &= -\hbar[\delta_0|2\rangle\langle 2| + \delta_2|3\rangle\langle 3| + \delta_1|4\rangle\langle 4| \\ &\quad +(G_2|2\rangle\langle 3| + G_1|2\rangle\langle 4| + H.c.)]\,, \end{aligned} \tag{73}$$

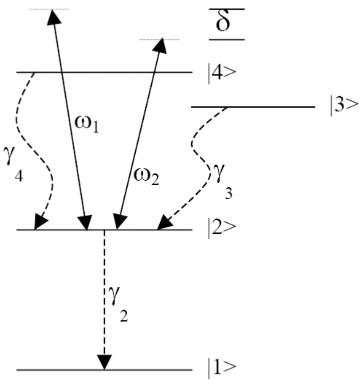

Fig. 8. Schematic diagram of a four-level Y-type system having two closely spaced uppermost levels interacting simultaneously with two independent coherent fields of frequencies ω_1 and ω_2. Frequency mismatch (δ) between the two fields is considered to introduce the dynamic phase-variation effect in the formation of the emission spectrum. γ_2, γ_3 and γ_4 are the decay rates of the excited levels.

where $G_1 = \bar{\mu}_{24}\bar{E}_1/(2\hbar)$ and $G_2 = \bar{\mu}_{23}\bar{E}_2/(2\hbar)$. The anomalous peak-shifting effect is introduced by the newly defined detuning terms as expressed below

$$\begin{aligned} \delta_0 &= \frac{|G'_1|^2 - |G'_2|^2}{\delta}\,, \\ \delta_1 &= \Delta_1 - \frac{|G'_1|^2}{\delta}\,, \\ \delta_2 &= \Delta_2 + \frac{|G'_2|^2}{\delta}\,, \end{aligned} \tag{74}$$

where $\delta = \omega_1 - \omega_2$, $G'_1 = \bar{\mu}_{24}.\bar{E}_2/(2\hbar)$, $G'_2 = \bar{\mu}_{23}.\bar{E}_1/(2\hbar)$, $\Delta_1 = \omega_1 - \omega_{42}$ and $\Delta_2 = \omega_2 - \omega_{32}$. To find the steady state spectrum, we follow the semiclassical density matrix approach as presented in Section 3.1. The relaxation terms, which need to be redefined in this formulation, are given as $\Gamma_{12} = \Lambda + \gamma_2/2 + i\delta_0$, $\Gamma_{23} = \Lambda/2 + (\gamma_2 + \gamma_3)/2 + i(\delta_2 - \delta_0)$, $\Gamma_{24} = \Lambda/2 + (\gamma_2 + \gamma_4)/2 + i(\delta_1 - \delta_0)$. The expression for the correlation function, as defined in Eq. (66), remains the same in the present formulation. Only the steady-state values of ρ_{22}, ρ_{23} and ρ_{24} are changed.

Numerical computation of the spectrum is carried out by choosing $G_1 = G_1'$ and $G_2 = G_2'$. In Fig. 9, we show the spectra for $\Lambda = 0.1\gamma$ and $\delta = 6\gamma$. When each of the two fields is exactly tuned to resonance with one of the excited levels such that $\Delta_1 = \Delta_2 = 0$, the three peak structure evolves in the spectrum, as shown by the curve a in Fig. 9. This spectral behaviour is completely different from the usual resonant characteristics of the spectrum obtained under the same condition of detuning as mentioned in Section 3.2, while for non-resonant detuning ($\Delta_1 = -\Delta_2 = 6\gamma$) of the fields, two peak spectrum is obtained as exhibited by the curve b. Thus, by changing the frequency mismatch between two coherent fields, spectral positions of the peaks can be shifted without any change in the values of Rabi frequencies in any of the two cases. The way of shifting is contrary to the usual peak-shifting effect introduced by the detuning terms Δ_1 and Δ_2 as studied in Section 3.2.

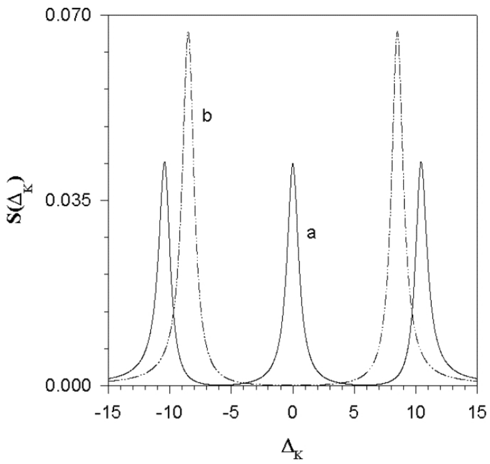

Fig. 9. Control of resonant and non-resonant evolution of spectral features via dynamic phase-variation effect. For $\delta = 6$, $G_1 = G_2 = 6$ and $\Lambda = 0.1$, we show the curve a ($\Delta_1 = \Delta_2 = 0$) and curve b ($\Delta_1 = -\Delta_2 = 6$). All rates are in units of γ_2.

Figures 10a-b exhibit a strong influence of the dynamic phase-variation effect on the emission spectrum when the incoherency effect on the spectrum is significant. The curve a of Fig. 10a is plotted for $\Delta_1 = \Delta_2 = 0$, $G_1 = 5.605\gamma$, $G_2 = 4\gamma$ and $\delta = 4\gamma$. For a comparison of the spectral behaviour, as represented by the curve a to that can be obtained without any inclusion of the frequency mismatch, we show the curve b in Fig. 10a with the same values of Rabi frequencies ($R_1 = G_1$ and $R_2 = G_2$). For the curve b, the values of detuning parameters are set to be equal to

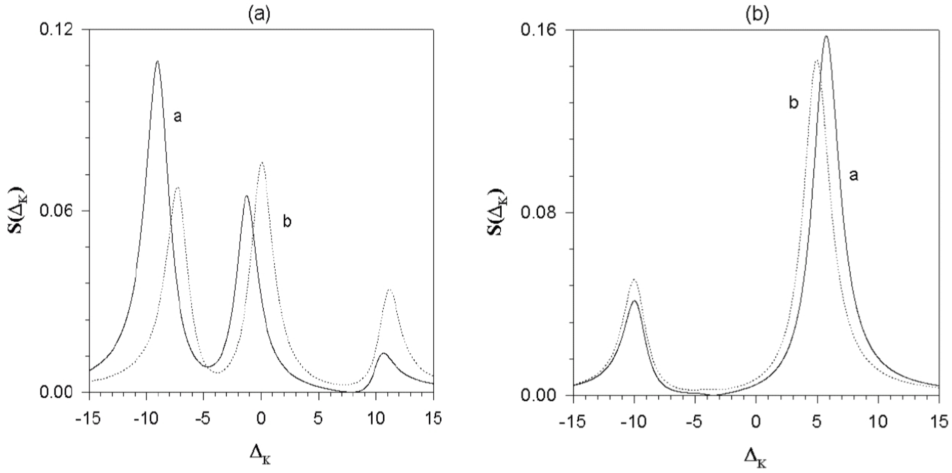

Fig. 10. Controlling selective quenching of emission via dynamic phase-variation effect. For $\Lambda = 1$, we show (a) the curves a ($\Delta_1 = \Delta_2 = 0$, $G_1 = 5.605$, $G_2 = 4$ and $\delta = 4$), and b ($\Delta_1 = \delta_1$, $\Delta_2 = \delta_2$ [δ_1 and δ_2 are calculated from Eq. (74) for $\Delta_1 = \Delta_2 = 0$], $G_1 = 5.605$, $G_2 = 4$); (b) the curves a ($\Delta_1 = \Delta_2 = 4$, $G_1 = 4$, $G_2 = 5.84$ and $\delta = 20$) and b ($\Delta_1 = \delta_1$, $\Delta_2 = \delta_2$ [δ_1 and δ_2 are calculated from Eq. (74) for $\Delta_1 = \Delta_2 = 4$], $G_1 = 4$, $G_2 = 5.84$). All rates are in the units of γ_2.

δ_j ($j = 1, 2$) which appear at the detuning condition of curve a. It is noticeable that the dynamic phase-variation effect introduces the shifting of peaks with selective quenching of the emission within the spectral line shape when $\Lambda = \gamma$. In Fig. 10b, similar spectral behaviour is also depicted by the two peak spectrum shown in curve a ($\Delta_1 = \Delta_2 = 4\gamma$, $G_1 = 4\gamma$, $G_2 = 5.84\gamma$, $\delta = 20\gamma$ and $\Lambda = \gamma$) when it is compared to the curve b ($\Delta_1 = \delta_1$, $\Delta_2 = \delta_2$, $R_1 = G_1$, $R_2 = G_2$ and $\Lambda = \gamma$).

7. *Conclusion*

The resonant and non-resonant evolution of spontaneous emission spectra have been studied in an ideal Y-type model. It has been shown that complete cancellation of spontaneous emission can be obtained in our model. The coherent features have been analyzed by using the dressed-state model. Considering the system under purely dissipative environment, for different dynamic conditions, we discussed the coherent control of the spectral behaviour. The required conditions of achieving subnatural linewidths of the spectral lines have been predicted. For unequal decay rates of the excited states $|3\rangle$ and $|4\rangle$, we have shown that the phenomenon of constructive quantum interference can strongly modify the emission line shape at the condition of non-resonant detuning of the fields. In such a condition, due to the phenomenon of quantum interference, two distinct peaks disappear at their spectral positions and a new peak results in the line shape at a different spectral position. We have shown the dependence of the line intensities on the incoherent pumping rates.

For a specific field configuration in the present model, the static phase-variation effect arising from the mutual orientation of the field polarizations is investigated to exhibit the phase-dependent control of emission spectrum. For two coherent fields of same static phase, but of different frequencies, the dynamic phase-variation effect can be introduced by the frequency mismatch between the fields. Depending on the values of the frequency mismatch, anomalous peak-shifting effect is displayed by the emission spectra in different dynamic conditions. The peak-shifting effect is accompanied by the selective quenching of emission within the spectral profile.

References

[1] E. Arimondo, *Progress in Optics*, Vol. 35, ed. E. Wolf, Elsevier, Amsterdam (1996).

[2] M. Fleischhauer, A. Imamoglu and J. P. Marangos, Rev. Mod. Phys. **77** (2005) 633; X. M. Hu and J. S. Peng, J. Phys. B: At Mol. Opt. Phys. **33** (2000) 921; M. Fleischhauer, C. H. Keitel, L. M. Narducci, M. O. Scully, S. Y. Zhu and M. S. Zubairy, Opt. Commun. **94** (1992) 599.

[3] G. S. Agarwal, Phys. Rev. A **55** (1997) 2467; Y. -Q. Li, and M. Xiao, Phys. Rev. A **51** (1995) 4959; H. Y. Ling, Y.-Q. Li and M. Xiao, Phys. Rev. A **53** (1996) 1014.

[4] S. E. Harris, Phys. Today **50** (1997) 36; J. P. Marangos, J. Mod. Opt. **45** (1998) 471; D. J Fulton, S. Shepherd, R. R. Moseley, B. D. Sinclair and M. H. Dunn, Phys. Rev. A **52** (1995) 2302; S. Wielandy and A. L. Gaeta, Phys. Rev. A **58** (1998) 2500.

[5] A. Imamoglu, J. E. Field and S. E. Harris, Phys. Rev. Lett. **66** (1991) 1154; J. Mompart and R. Corbalan, J. Opt. B: Quantum Semiclass. Opt. **2** (2000) R7; A. S. Zibrov, M. D. Lukin, D. E. Nikonov, L. Hollberg, M. O. Scully, V. L. Velichansky and H. G. Robinson, Phys. Rev. Lett. **75** (1995) 1499; B. K. Dutta and P. K. Mahapatra, Phys. Scr. **77** (2008) 025403.

[6] M. O. Scully and S. Y. Zhu, Opt. Commun. **87** (1992) 134; M. Fleischhauer, C. H. Keitel, M. O. Scully, C. Su, B. T. Ulrich and S. Y. Zhu, Phys. Rev. A **46** (1992) 1468.

[7] G. S. Agarwal and W. Harshawarbhan, Phys. Rev. Lett. **77** (1996) 1039.

[8] N. Mulchan, D. G. Ducreay, R. Pina, M. Yan and Y. Zhu, J. Opt. Soc. Am. B **17** (2000) 820.

[9] S. E. Harris and H. Yamamoto, Phys. Rev. Lett. **81** (1998) 3611.

[10] Y. Wu, J. Saldana and Y. Zhu, Phys. Rev. A **67** (2003) 013811; B. K. Dutta and P. K. Mahapatra, Phys. Scr. **75** (2007) 345.

[11] P. R. Berman, Phys. Rev. A **58** (1998) 4886.

[12] F. Ghafoor, S. Y. Zhu and M. S. Zubairy, Phys. Rev. A **62** (2000) 013811.

[13] J. H. Wu, A. J. Li, Y. Ding, Y. C. Zhao and J. Y. Gao, Phys. Rev. A **72** (2005) 023802.

[14] A. J. Li, J. Y. Gao, J. H. Wu and L. Wang, J. Phys. B: At Mol. Opt. Phys. **38** (2005) 3815.

[15] J. H. Li, A. X. Chen, J. B. Liu and X. Yang, Opt. Commun. **278** (2007) 124.

[16] T. Quang, M. Boldeyohannes, S. John and G. S. Agarwal, Phys. Rev. Lett. **81** (1998) 3611.

[17] B. P. Hou, S. J. Wang, W. L. Yu and W. L. Sun, Phys. Rev. A **69** (2004) 053805; B. P. Hou, S. J. Wang, W. L. Yu and W. L. Sun, J. Phys. B: At. Mol. Opt. Phys. **38** (2005) 1419.

[18] J. Y. Gao, S. H. Yang, D. Wang, X. Z. Guo, K. X. Chen, Y. Jiang and B. Zhao, Phys. Rev. A **61** (2000) 023401; D. Wang, J. Y. Gao, J. H. Xu, G. C. La Rocca and F. Bassani, Europhys. Lett. **54** (2001) 456; J. H. Xu, G. C. La Rocca, F. Bassani, D. Wang and J. Y. Gao, Opt. Commun. **216** (2003) 157.

[19] B. K. Dutta and P. K. Mahapatra, J. Phys. B: At Mol. Opt. Phys. **41** (2008) 055501.

[20] R. Arun, arxiv:0710.1388v1 [quant.ph], (2007).

[21] P. R. Fontana and R. P. Srivastava, Phys. Rev. A **7** (1973) 1866.

[22] S. Y. Zhu, L. M. Narducci and M. O. Scully, Phys. Rev. A **52** (1995) 4791.

[23] S. Yuan and J. Y. Gao, Eur. Phys. J. D **11** (2000) 267.

[24] F. Plastina and F. Piperno, Phys. Lett. A **236** (1997) 16.

[25] J. Liu, Z. Zhang, G. Xiao and C. P. Grover, J. Opt. B: Quantum Semiclass. Opt. **5** (2003) S633.

[26] D. A. Cardimona, M. G. Raymer and C. R. Stroud Jr, J. Phys. B: At. Mol. Opt. Phys. **15** (1982) 55; J. Javanainen, Europhys. Lett. **17** (1992) 407; Z. Ficek and S. Swain, J. Mod. Opt. **49** (2002) 3; A. Joshi, W. Yang and M. Xiao, Phys. Lett. A **325** (2004) 30.

[27] D. Agassi, Phys. Rev. A **30** (1984) 2449; S. Y. Zhu, R. C. F. Chan and C. P. Lee, Phys. Rev. A **52** (1995) 710; S. Y. Zhu and M. O. Scully, Phys. Rev. Lett. **76** (1996) 388.

[28] H. Lee, P. Polypkin, M. O. Scully and S. Y. Zhu, Phys. Rev. A **55** (1997) 4454.

[29] F. Plastina and F. Piperno, Phys. Rev. A **62** (2000) 053801.

[30] S. Y. Zhu, Quantum. Opt. **7** (1995) 385; H. Huang, S. Y. Zhu and M. S. Zubairy, Phys. Rev. A **55** (1997) 744.

[31] B. K. Dutta and P. K. Mahapatra, Opt. Commun. **282** (2009) 594.

[32] H. R. Xia, C. Y. Ye and S. Y. Zhu, Phys. Rev. Lett. **77** (1996) 1032.

[33] E. Paspalakis, C. H. Keitel and P. L. Knight, Phys. Rev. A **58** (1998) 4868.

[34] M. A. G. Martinez, P. R. Herczfeld, C. Samuels, L. M. Narducci and C. H. Keitel, Phys. Rev. A **55** (1997) 4483.

[35] J. H. Li, Eur. Phys. J. D **42** (2007) 467.

[36] J. H. Li, J. B. Liu, A. X. Chen and C. C. Qi, Phys. Rev. A **74** (2006) 033816.

[37] M. O. Scully and M. S. Zubairy, *Quantum Optics*, Cambridge University Press, Cambridge (1997).

[38] K. T. Kapale, M. O. Scully, S. Y. Zhu and M. S. Zubairy, Phys. Rev. A **67** (2003) 023804.

[39] S. M. Bernett and P. M. Radmore, *Methods in Theoretical Quantum Optics*, Oxford University Press, Oxford (1997).

[40] Z. Ficek and S. Swain, *Quantum Interference and Coherence*, Springer Series in Optical Sciences, Springer, USA (2005).

[41] S. E. Harris, J. E. Field and A. Imamoglu, Phys. Rev. Lett. **64** (1990) 1107.

[42] B. R. Mollow, Phys. Rev. A **5** (1972) 1522; G. S. Agarwal. Phys. Rev. A **54** (1996) R3734.

KOHERENTNO UPRAVLJANJE SPEKTROM SPONTANE EMISIJE U DVOJNO TJERANOM ATOMU TIPA Y

Proučavamo dinamičko upravljanje spektrom spontane emisije atomskog sustava tipa Y koji tjeraju dva koherentna polja. Proučavamo ovisnost svojstava koherentnog spektra o različitim uvjetima, u oguljenom sustavu i primjenom potpunog sustava. Ako sustav troši energiju, onda svojstvima spektralnih sastavnica možemo koherentno upravljati mijenjanjem Rabijevih frekvencija i narušavanjem ugodbe vanjskih polja. Uz uvjet rezonantnog razvoja spektra, pokazujemo kako se oblik emisijske linije može jako promijeniti uz nejednoliko raspadanje gornjeg dubleta. U tim uvjetima konstruktivna kvantna interferencija uzrokuje nastanak jednog vrha na određenom mjestu u spektru kada dva jasna vrha nestanu u drugim dijelovima spektra. Radi međusobne orijentacije polarizacija polja koja djeluju na atom u nekom stanju, uključili smo i učinak promjene statičke faze da bismo prikazali faznoovisne spektre. Ovaj model predstavljamo s tipičnim oblikom polja tako da nesklad frekvencija dovodi do dinamičkih promjena faze. Ta pojava vodi na anomalne pomake vrhova i mogućnost odabira gušenja emisije unutar spektralnog područja.